Eu^{2+}-activated silicon-oxynitride $Ca_3Si_2O_4N_2$: a green-emitting phosphor for white LEDs

Yi-Chen Chiu,[1,*] Chien-Hao Huang,[2] Te-Ju Lee,[2] Wei-Ren Liu,[1] Yao-Tsung Yeh,[1] Shyue-Ming Jang,[1] and Ru-Shi Liu[3,*]

[1]*Material and Chemical Research Laboratories, ITRI, Hsinchu 300, Taiwan*
[2]*Phosphors Research Laboratory and Department of Applied Chemistry, National Chiao Tung University, Hsinchu 300, Taiwan*
[3]*Department of Chemistry, National Taiwan University, Taipei 106, Taiwan*
**marmaidtw@itri.org.tw; rsliu@ntu.edu.tw*

Abstract: The green-emitting phosphor $Ca_3Si_2O_4N_2:Eu^{2+}$ was synthesized using a solid-state reaction. The luminescence properties, diffuse reflection spectrum, and thermal quenching were firstly studied, and a white light-emitting diode (wLED) was fabricated using the Eu^{2+}-activated $Ca_3Si_2O_4N_2$ phosphor. Eu^{2+}-doped $Ca_3Si_2O_4N_2$ exhibited a broad green emission band centered between 510 and 550 nm depending on the concentration of Eu^{2+}. The optimal doping concentration of Eu^{2+} in $Ca_3Si_2O_4N_2$ was 1 mol%. The energy transfer between Eu^{2+} ions proceeds by an electric multipolar interaction mechanism, with a critical transfer distance of approximately 30.08 Å. A wLED with an color-rendering index R_a of 88.25 at a correlated color temperature of 6029 K was obtained by combining a GaN-based *n*-UV LED (380 nm) with the blue-emitting $BaMgAl_{10}O_{17}:Eu^{2+}$, green-emitting $Ca_3Si_2O_4N_2:Eu^{2+}$, and red-emitting $CaAlSiN_3:Eu^{2+}$ phosphors. The results present $Ca_3Si_2O_4N_2:Eu^{2+}$ as an attractive candidate for use as a conversion phosphor for wLED applications.

OCIS codes: (160.2540) Fluorescent and luminescent materials; (250.5230) Photoluminescence; (300.6280) Spectroscopy, fluorescence and luminescence.

References and links

1. W. B. Im, Y. I. Kim, N. N. Fellows, H. Masui, G. A. Hirata, S. P. DenBaars, and R. Seshadri, "A yellow-emitting Ce^{3+} phosphor, $La_{1-x}Ce_xSr_2AlO_5$, for white light-emitting diodes," Appl. Phys. Lett. **93**(9), 091905 (2008).
2. T. Nishida, T. Ban, and N. Kobayashi, "High-color-rendering light sources consisting of a 350-nm ultraviolet light-emitting diode and three-basal-color phosphors," Appl. Phys. Lett. **82**(22), 3817–3819 (2003).
3. S. Nakamura, T. Mukai, and M. Senoh, "Candela-class high-brightness InGaN/AlGaN double-heterostructure blue-light-emitting diodes," Appl. Phys. Lett. **64**(13), 1687–1689 (1994).
4. S. Ye, F. Xiao, Y. X. Pan, Y. Y. Ma, and Q. Y. Zhang, "Phosphors in phosphor-converted white light-emitting diodes: Recent advances in materials, techniques and properties," Mater. Sci. Eng. Rep. **71**(1), 1–34 (2010).
5. H. A. Höppe, H. Lutz, P. Morys, W. Schnick, and A. Seilmeier, "Luminescence in Eu^{2+}-doped $Ba_2Si_5N_8$: fluorescence, thermoluminescence, and upconversion," J. Phys. Chem. Solids **61**(12), 2001–2006 (2000).
6. Y. Q. Li, G. de With, and H. T. Hintzen, "Luminescence properties of Ce3+-activated alkaline earth silicon nitride $M_2Si_5N_8$ (M = Ca, Sr, Ba) materials," J. Lumin. **116**(1-2), 107–116 (2006).
7. R. J. Xie, N. Hirosaki, T. Suehiro, F. F. Xu, and M. Mitomo, "A Simple, Efficient Synthetic Route to $Sr_2Si_5N_8:Eu^{2+}$-Based Red Phosphors for White Light-Emitting Diodes," Chem. Mater. **18**(23), 5578–5583 (2006).
8. Y. Q. Li, G. de With, and H. T. Hintzen, "The effect of replacement of Sr by Ca on the structural and luminescence properties of the red-emitting $Sr_2Si_5N_8:Eu^{2+}$ LED conversion phosphor," J. Solid State Chem. **181**(3), 515–524 (2008).
9. K. S. Sohn, B. Lee, R. J. Xie, and N. Hirosaki, "A Rate Equation Model for Energy Transfer between Activators at Different Crystallographic Sites in $Sr_2Si_5N_8:Eu^{2+}$," Opt. Lett. **34**(21), 3427–3429 (2009).
10. K. Uheda, N. Hirosaki, Y. Yamamoto, A. Naito, T. Nakajima, and H. Yamamoto, "Luminescence Properties of a Red Phosphor, $CaAlSiN_3:Eu^{2+}$, for White Light-Emitting Diodes," Electrochem. Solid-State Lett. **9**(4), H22–H25 (2006).
11. H. Watanabe, H. Wada, K. Seki, M. Itou, and N. Kijima, "Synthetic Method and Luminescence Properties of $Sr_xCa_{1-x}AlSiN_3:Eu^{2+}$ Mixed Nitride Phosphors," J. Electrochem. Soc. **155**(3), F31 (2008).
12. X. Piao, K. Machida, T. Horikawa, H. Hanzawa, Y. Shimomura, and N. Kijima, "Preparation of $CaAlSiN_3:Eu^{2+}$ phosphors by the self-propagating high-temperature synthesis and their luminescent properties," Chem. Mater. **19**(18), 4592–4599 (2007).

#145127 - $15.00 USD Received 31 Mar 2011; revised 27 Apr 2011; accepted 27 Apr 2011; published 28 Apr 2011

13. S. Lee, and K. S. Sohn, "The effect of Inhomogeneous Broadening on Time-Resolved Photoluminescence in $CaAlSiN_3:Eu^{2+}$," Opt. Lett. **35**(7), 1004–1006 (2010).
14. Y. W. Jung, B. Lee, S. P. Singh, and K. S. Sohn, "Particle-swarm-optimization-assisted rate equation modeling of the two-peak emission behavior of non-stoichiometric $CaAl_{(x)}Si_{((7-3x)/4)}N_3:Eu^{2+}$ phosphors," Opt. Express **18**(17), 17805–17818 (2010).
15. Y. Q. Li, C. M. Fang, G. de With, and H. T. Hintzen, "Preparation,structure and photoluminescence properties of Eu^{2+} and Ce^{3+}-doped $SrYSi_4N_7$," J. Solid State Chem. **171** (12), 4687–4694 (2004).
16. Y. Q. Li, G. de With, and H. T. Hintzen, "Synthesis, structure, and luminescence properties of Eu^{2+} and Ce^{3+} activated $BaYSi_4N_7$," J. Alloy. Comp. **385**(1-2), 1–11 (2004).
17. C. Kulshreshtha, J. H. Kwak, Y. J. Park, and K. S. Sohn, "Photoluminescent and decay behaviors of Mn^{2+} and Ce^{3+} co-activated $MgSiN_2$ phosphors for use in LED applications," Opt. Lett. **34**(6), 794–796 (2009).
18. R. S. Liu, Y. H. Liu, N. C. Bagkar, and S. F. Hua, "Enhanced luminescence of $SrSi_2O_2N_2:Eu^{2+}$ phosphors by codoping with Ce^{3+}, Mn^{2+}, and Dy^{3+} ions," Appl. Phys. Lett. **91**, 061119 (2007).
19. Y. Q. Li, A. C. A. Delsing, G. de With, and H. T. Hintzen, "Luminescence Properties of Eu^{2+}-Activated Alkaline-Earth Silicon-Oxynitride $MSi_2O_{2-\delta}N_{2+2/3\delta}$ (M = Ca, Sr, Ba): A Promising Class of Novel LED Conversion Phosphors," Chem. Mater. **17**(12), 3242–3248 (2005).
20. T. Suehiro, N. Hirosaki, R. J. Xie, and M. Mitomo, "Powder Synthesis of Ca-α'-SiAlON as a Host Material for Phosphors," Chem. Mater. **17**(2), 308–314 (2005).
21. K. Sakuma, N. Hirosaki, R. J. Xie, Y. Yamamoto, and T. Suehiro, "Luminescence properties of (Ca,Y)-α-SiAlON:Eu phosphors," Mater. Lett. **61**(2), 547–550 (2007).
22. R. J. Xie, K. Kimoto, T. Sekiguchi, Y. Yamamoto, T. Suehiro, M. Mitomo, and N. Hirosaki, "Characterization and properties of green-emitting β-SiAlON:Eu^{2+} powder phosphors for white light-emitting diodes," Appl. Phys. Lett. **86**(21), 211905 (2005).
23. Z. K. Huang, W. Y. Sun, and D. S. Yan, "Phase relations of the Si_3N_4-AIN-CaO system," J. Mater. Sci. Lett. **4**(3), 255–259 (1985).
24. A. Sharafat, "Preparation, characterization and properties of nitrogen rich glasses in alkaline earth-Si-O-N systems," Ph. D. Thesis, Stockholm University, (2009).
25. W. R. Liu, Y. C. Chiu, C. Y. Tung, Y. T. Yeh, S. M. Jang, and T. M. Chen, "A Study on the Luminescence Properties of $CaAlBO_4:RE^{3+}$ (RE = Ce, Tb, and Eu) Phosphors," J. Electrochem. Soc. **155**(9), J252–J255 (2008).
26. P. Mondal, and J. W. Jeffery, "The crystal structure of tricalcium aluminate, $Ca_3Al_2O_6$," Acta Crystallogr. B **31**(3), 689–697 (1975).
27. R. D. Shannon, "Revised effective ionic radii and systematic studies of interatomic distances in halides and chalcogenides," Acta Crystallogr. A **32**(5), 751–767 (1976).
28. G. Blasse, "Energy transfer in oxidic phosphors," Philips Res. Rep. **24**, 131 (1969).
29. D. L. Dexter, "A Theory of Sensitized Luminescence in Solids," J. Chem. Phys. **21**(5), 836–850 (1953).
30. L. G. Van Uitert, "Characterization of Energy Transfer Interactions between Rare Earth Ions," J. Electrochem. Soc. **114**(10), 1048–1053 (1967).

1. Introduction

In recent years, there has been considerable interest in white light-emitting diodes (wLEDs) owing to their long operation lifetime, low energy consumption, high material stability, and environmentally friendly characteristics [1–4]. These desirable characteristics may ultimately lead to the replacement of gas-discharge fluorescent lamps by wLEDs in the near future. In general, white light can be generated by a combination of blue LED chips coated with the yellow-emitting phosphor $Y_3Al_5O_{12}:Ce^{3+}$ ($YAG:Ce^{3+}$). Nevertheless, the drawbacks of this method include a low-rendering index and a high color temperature due to the deficiency of red emission in the visible spectrum. The alternative approach to generating white light involves combining a near ultraviolet (n-UV) LED (380–420nm) with RGB (red, green, blue) phosphors. Consequently, the development of new phosphors that can be effectively excited in the near ultraviolet range is an important prospect that requires prompt attention.

Nitride/oxynitride hosts such as $M_2Si_5N_8$ (M = Ca, Sr, Ba) [5–9], $MAlSiN_3$ (M = Ca, Sr) [10–14], $MYSi_4N_7$ (M = Sr, Ba) [15,16], $MgSiN_2$ [17], $MSi_2O_2N_2$ (M = Ca, Sr, Ba) [18,19], α-SiAlON [20,21], and β-SiAlON [22], which present intense luminescence when activated with Eu^{2+}, are good candidates for host materials owing to several merits such as their high chemical and physical stability and low thermal quenching. The powder X-ray data of $Ca_3Si_2O_4N_2$ was first reported by Huang *et al*. [23] Sharafat later reported the crystal structure of $Ca_{3-x}Si_2O_{4+2x}N_{2-2x}$ [24]. The luminescence properties of $Ca_3Si_2O_4N_2$, however, have not been previously investigated, to the best of our knowledge. In the present study, the luminescence properties, thermal stability, and application of the green-emitting $Ca_3Si_2O_4N_2:Eu^{2+}$ phosphors in the fabrication of a wLED by combination with a n-UV LED are investigated. The results show that $Ca_3Si_2O_4N_2:Eu^{2+}$ has good thermal stability, and the

#145127 - $15.00 USD Received 31 Mar 2011; revised 27 Apr 2011; accepted 27 Apr 2011; published 28 Apr 2011

white LEDs fabricated using $Ca_3Si_2O_4N_2:Eu^{2+}$ exhibit high CRI. The green-emitting phosphor based on $Ca_3Si_2O_4N_2:Eu^{2+}$ is a promising candidate for solid-state lighting applications.

2. Experimental

The polycrystalline phosphors composed of $Ca_3Si_2O_4N_2:Eu^{2+}$ were prepared by a solid-state reaction in which the constituent raw materials $CaCO_3$ (99.99%), α-Si_3N_4 (99.99%), SiO_2 (99.6%), and Eu_2O_3 (99.99%) (all from Aldrich Chemicals, Milwaukee, WI, U.S.A) were weighed in stoichiometric proportions. The powder mixtures were sintered under a reducing atmosphere (15%H_2/85%N_2) at 1400°C for 8 h with one intermittent regrinding to prevent the possibility of incomplete reaction. The products were then cooled to room temperature in the furnace, ground, and pulverized for further measurements. Powder X-ray diffraction (XRD) of the samples was performed using a Bruker AXS D8 advanced automatic diffractometer with Cu-K_α radiation (λ = 1.5418 Å), operating at 40 kV and 30 mA. The XRD profiles were collected in the range of $10° < 2\theta < 80°$. The photoluminescence (PL) and photoluminescence excitation (PLE) spectra were measured at room temperature using a Spex Fluorolog-3 spectrofluorometer (Instruments S.A., N.J., U.S.A) equipped with a 450 W Xe light source and double excitation monochromators. The quantum efficiency (QE) was measured by an integrating sphere whose inner face was coated with Spectralon equipped with a spectrofluorometer (Horiba Jobin-Yvon Fluorolog 3–22 Tau-3). The measurement procedures and correlation theorem were described previously by Liu et al. [25] The Commission International de I'Eclairage (CIE) chromaticity coordinates for all samples were determined using a Laiko DT-100 color analyzer equipped with a CCD detector (Laiko Co., Tokyo, Japan). The diffuse reflection spectra were recorded in the range of 200–800 nm with a Hitachi 3010 double-beam UV-VIS spectrometer (Hitachi Co., Tokyo, Japan) equipped with a Ø60 mm integrating sphere whose inner face was coated with $BaSO_4$ or Spectralon and PTFE.

3. Results and discussion

3.1. Crystal Structure of $Ca_3Si_2O_4N_2$

Figure 1 shows the X-ray powder diffraction (XRD) pattern of the as-synthesized $Ca_3Si_2O_4N_2$:9%Eu^{2+} powder. The as-prepared $Ca_3Si_2O_4N_2$ material was obtained as a single phase compound that matches well with JCPDS file No. 38-0944. From the single crystal X-ray data reported by Sharafat [24], $Ca_{2.88}Si_2O_{4.23}N_{1.77}$ crystallizes in the cubic space group $Pa\bar{3}$ with unit cell dimensions of $a = b = c = 15.07$Å and with twenty-four formula units per unit cell. The crystal structure of $Ca_3Si_2O_4N_2$, which is similar to that of $Ca_3Al_2O_6$ [26], is shown in Fig. 2. The crystal structure of $Ca_3Si_2O_4N_2$ consists of isolated 12-membered rings composed of $Si_{12}(O,N)_{36}$. Seven different crystallographic sites are available for the Ca^{2+} ions, which are located in the voids of the packed 12-membered rings. The effective cationic radii (r) reported by Shannon [27] indicate that the ionic radius of Eu^{2+} is close to that of Ca^{2+}. Based on size considerations, it was expected that upon doping, the Eu^{2+} cation would occupy the Ca^{2+} lattice site given that the Si^{4+} site is too small for Eu^{2+} to occupy.

#145127 - $15.00 USD Received 31 Mar 2011; revised 27 Apr 2011; accepted 27 Apr 2011; published 28 Apr 2011

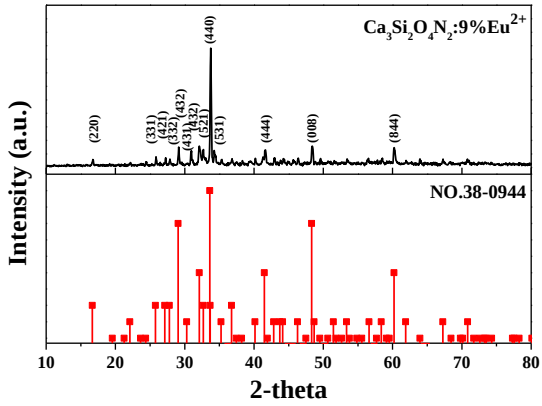

Fig. 1. XRD patterns of $Ca_3Si_2O_4N_2$ (JCPDS 38-0944) and $Ca_3Si_2O_4N_2$:9%Eu^{2+} samples.

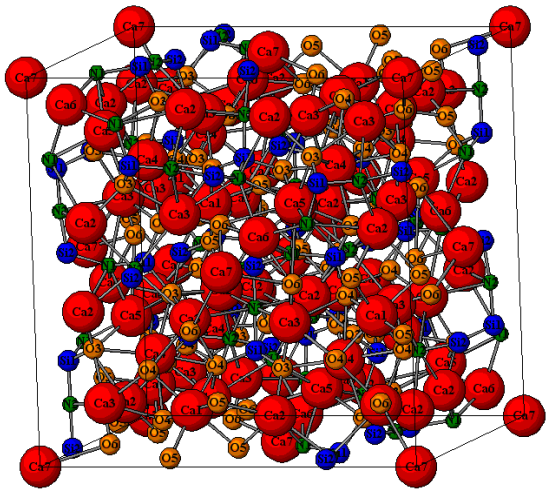

Fig. 2. Crystal structure of $Ca_3Si_2O_4N_2$.

3.2. Photoluminescence Properties of $Ca_3Si_2O_4N_2$:Eu^{2+}

Figure 3 shows the excitation and emission spectra of $Ca_3Si_2O_4N_2$:Eu^{2+} for different Eu^{2+} concentrations. The excitation bands of the samples doped with varying concentrations of Eu^{2+} had peaks at ~289 nm, ~328 nm, ~368 nm, and ~405 nm, which consisted mainly of unresolved bands of the $4f^6 5d^1$ multiplets of the Eu^{2+} excited states. The sample exhibited a green emission band with maximum emission at 510 nm, under optimal excitation at 330 nm. Although the excitation maximum was obtained at 330 nm, the samples could be efficiently excited in the range of 350–400 nm. Consequently, an n-UV chip (380 nm) was selected for use in the subsequent fabrication of the white LEDs. A broad, asymmetric band was observed in the emission spectrum in the wavelength range of 450–650 nm, which corresponds to the allowed $4f^6 5d^1 \rightarrow 4f^7$ electronic transitions of Eu^{2+}. The broad excitation band was attributed to the high covalency of the Ca_{Eu}-N bond and a large crystal-field splitting effect. The crystal-field splittings of Eu^{2+} shown in Table 1 were estimated to be 18730~21050 cm^{-1} in $Ca_3Si_2O_4N_2$. The Stokes shifts of $Ca_3Si_2O_4N_2$:x%Eu^{2+} (x = 0.0025–0.09) were estimated to be 10973 cm^{-1}–12500 cm^{-1}. The emission band shifts toward longer wavelength as the

#145127 - $15.00 USD Received 31 Mar 2011; revised 27 Apr 2011; accepted 27 Apr 2011; published 28 Apr 2011

concentration of the Eu^{2+} dopant increases. This bathochromic shift is ascribed to the change in the crystal-field splitting of Eu^{2+}. Consequently, the phenomenon can be explained in terms of energy transfer from Eu^{2+} ions at the higher 5*d* levels to those at the lower levels. This causes the emission energy from the 5*d* excited state to the 4*f* ground state to become lower, and therefore, the emission shifts to longer wavelength.

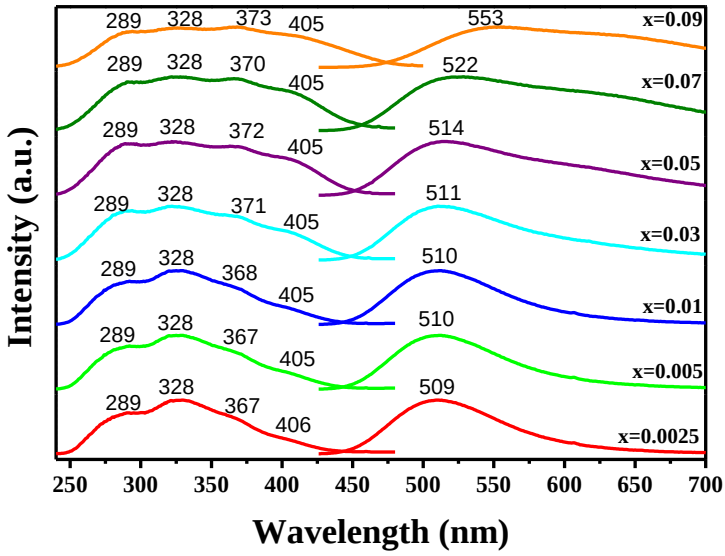

Fig. 3. Excitation and emission spectra of $Ca_3Si_2O_4N_2:Eu^{2+}$ with varying Eu^{2+} concentrations.

Table 1. Emission, Stokes Shift, Crystal Filed Splitting, Normalized PL Intensity and the CIE Coordinates for $(Ca_{1-x}Eu_x)_3Si_2O_4N_2$.

x	λ_{em} (nm)	Stokes shift (cm^{-1})	Crystal field splitting (cm^{-1})	Normalized PL intensity (%)	CIE (*x*, *y*)
0.0025	509	10841	18939	87	(0.25, 0.50)
0.0050	510	10879	19244	94	(0.26, 0.50)
0.0100	510	10849	19494	100	(0.26, 0.51)
0.0300	511	10918	20068	93	(0.29, 0.49)
0.0500	514	11032	20161	84	(0.33, 0.51)
0.0700	522	11330	20435	50	(0.35, 0.52)
0.0900	553	12403	21258	49	(0.42, 0.52)

Figure 4 shows the PL intensity of $Ca_3Si_2O_4N_2:Eu^{2+}$ as a function of doped Eu^{2+} content. The optimal doping concentration was observed at 1 mol%, the PL intensity was found to decline dramatically as the content of Eu^{2+} exceeds 1 mol% due to concentration quenching. Concentration quenching is mainly caused by energy transfer among Eu^{2+} ions, the possibility of which increases as the concentration of Eu^{2+} increases. Blasse [28] pointed out that the

#145127 - $15.00 USD Received 31 Mar 2011; revised 27 Apr 2011; accepted 27 Apr 2011; published 28 Apr 2011

critical transfer distance (R_c) is approximately equal to twice the radius of a sphere with the volume of the unit cell:

$$Rc = 2\left[\frac{3V}{4\pi x_c Z}\right]^{1/3}, \quad (1)$$

where x_c is the critical concentration, Z is the number of formula units per unit cell, and V is the volume of the unit cell. By taking the value of V = 3417.45 Å^3, Z = 24, and x_c = 0.01, the critical transfer distance R_c was found to be ~30.08 Å.

Non-radiative energy transfer from one Eu^{2+} ion to another Eu^{2+} ion may take place via an exchange interaction, radiation reabsorption, or an electric multipolar interaction. The exchange interaction requires a large direct or indirect overlap of the wavefunctions of the donor and acceptor, and this mechanism is responsible for energy transfer in the case of forbidden transitions. The critical distance for the exchange interaction is approximately 5 Å.[24] The $4f^7 \rightarrow 4f^6 5d^1$ transition of Eu^{2+} is allowed; hence, the exchange mechanism plays no role in the energy transfer within the $Ca_3Si_2O_4N_2$:Eu^{2+} phosphors. The mechanism of radiation reabsorption is only effective when the fluorescence and absorption spectra are broadly overlapping. Therefore, radiation reabsorption does not occur in this case. The process of energy transfer between Eu^{2+} ions in the $Ca_3Si_2O_4N_2$:Eu^{2+} phosphor is attributed to the electric multipolar interaction, as suggested by Dexter [29].

The emission intensity (I) per activator concentration (x) can be expressed by the following equation [29,30]:

$$\frac{I}{x} = \frac{k}{1+\beta(x)^{\theta/3}}, \quad (2)$$

where k and β are constants for each type of interaction for a given host lattice; θ = 6, 8, 10 for dipole–dipole, dipole–quadrupole, quadrupole–quadrupole interactions, respectively. The inset of Fig. 4 illustrates the I/x dependence on x on a logarithmic scale. The dependence of log (I/x) on log (x) was found to be relatively linear, and the slope was determined to be –1.15. The value of θ was found to be approximately 6, indicating that the concentration quenching mechanism of Eu^{2+} emission was dominated by the dipole–dipole interaction.

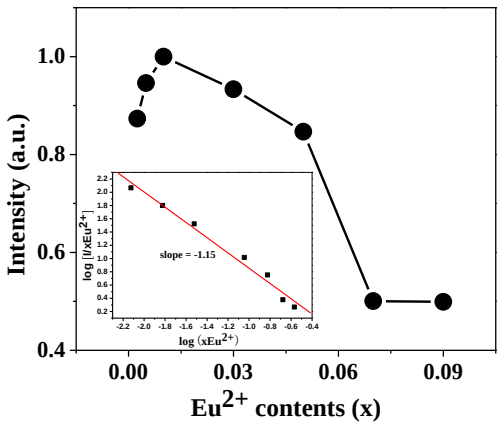

Fig. 4. Emission intensity of $Ca_3Si_2O_4N_2$ as a function of Eu^{2+} concentration. Inset: log(I/x_{Eu2+}) dependence of log(x_{Eu2+}).

The CIE chromaticity coordinates of the $Ca_3Si_2O_4N_2$ phosphors with different Eu^{2+} dopant contents are summarized in Table 1 and also shown in Fig. 5. The chromaticity index varies from (0.25, 0.50) for the composition with 0.25 mol% to (0.42, 0.52) for the composition with

#145127 - $15.00 USD Received 31 Mar 2011; revised 27 Apr 2011; accepted 27 Apr 2011; published 28 Apr 2011

9 mol%. The internal (η_i) and external (η_0) quantum efficiencies (QEs) were calculated based on the equations reported by Hirosaki et al. previously [22]. The internal quantum efficiency of $Ca_3Si_2O_4N_2$:Eu^{2+} and Ba_2SiO_4:Eu^{2+} phosphor were found to be 23.8% and 89.3% and the corresponding external quantum efficiency is 17.1% and 74.8%, respectively, at the excitation wavelength of 400 nm.

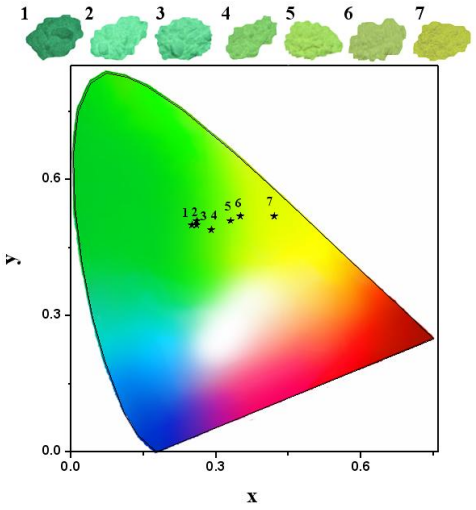

Fig. 5. CIE chromaticity diagram for $Ca_3Si_2O_4N_2$:Eu^{2+} phosphors with different Eu^{2+} dopant contents. The upper inset shows these phosphors under 365nm excitation in a UV box.

Figure 6 shows the diffuse reflectance spectra for the parent and the Eu^{2+}-doped $Ca_3Si_2O_4N_2$ phosphors. The daylight color of the undoped $Ca_3Si_2O_4N_2$ is white. Hence, the $Ca_3Si_2O_4N_2$ exhibited high reflectance in the UV to visible range (250–700 nm) and a decrease in reflectance in the 200–250 nm range, which corresponds to the host lattice absorption. Accordingly, the absorption edge of the undoped materials was estimated to be 245 nm (5.06 eV). The diffuse reflectance spectrum of the Eu^{2+}-doped $Ca_3Si_2O_4N_2$ shows an absorption band from 250 to 500 nm, which was attributed to the $4f \rightarrow 5d$ transition of Eu^{2+} in the $Ca_3Si_2O_4N_2$ matrix and which was consistent with the excitation spectrum.

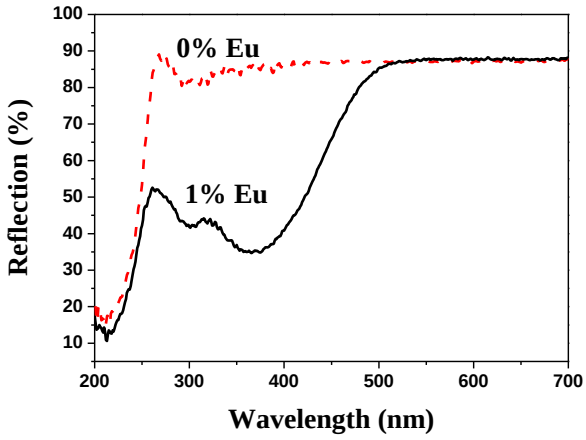

Fig. 6. Diffuse reflectance spectra of undoped (dashed line) and 1% Eu-doped (solid line) $Ca_3Si_2O_4N_2$.

#145127 - $15.00 USD Received 31 Mar 2011; revised 27 Apr 2011; accepted 27 Apr 2011; published 28 Apr 2011

3.3 Thermal Quenching Properties of $Ca_3Si_2O_4N_2:Eu^{2+}$

The thermal stability of phosphor is one of the major considerations for its application in high-power LEDs. The temperature dependence of the PL intensity of $Ca_3Si_2O_4N_2:Eu^{2+}$ under excitation at 380 nm and above room temperature is shown in Fig. 7. The activation energy (E_a) can be expressed by:

$$\ln(\frac{I_o}{I}) = \ln A - \frac{E_a}{kT}, \tag{3}$$

where I_o and I are the luminescence intensity of $Ca_3Si_2O_4N_2:Eu^{2+}$ at room temperature and the testing temperature, respectively; A is a constant, and k is Boltzmann's constant (8.617×10^{-5} eV K^{-1}). E_a was found to be 0.0687 eV. A comparison between the thermal quenching properties of $Ca_3Si_2O_4N_2:Eu^{2+}$ and $Ba_2SiO_4:Eu^{2+}$ (Fig. 7, inset) shows that the thermal quenching of $Ca_3Si_2O_4N_2:Eu^{2+}$ was superior to that of $Ba_2SiO_4:Eu^{2+}$. The results also indicate that $Ca_3Si_2O_4N_2:Eu^{2+}$ could be a promising phosphor for high-power LED applications.

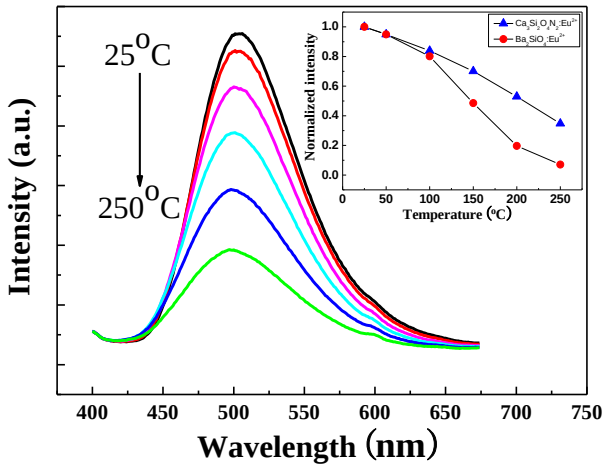

Fig. 7. Temperature-dependent emission spectra of $Ca_3Si_2O_4N_2:Eu^{2+}$ phosphor. Inset: normalized PL intensity as a function of temperature. For comparison, thermal quenching data of $Ba_2SiO_4:Eu^{2+}$ excited at 380 nm was also measured as a reference.

3.4 Electroluminescent Properties of $Ca_3Si_2O_4N_2:Eu^{2+}$

Figure 8 shows the spectrua of the white LED composed of an n-UV chip (380 nm) and blue ($BaMgAl_{10}O_{17}:Eu^{2+}$), green ($Ca_3Si_2O_4N_2:Eu^{2+}$) and red ($CaAlSiN_3:Eu^{2+}$) phosphors. An emitter-type LED package was chosen for the fabrication of the LED device on the basis of its high light extraction efficiency. The CIE color coordinates and correlated color temperature (CCT) of the white LED were found to be (0.322, 0.330) and 6029 K, respectively. The average color-rendering index, *Ra*, was determined to be 88.25, which was considered to be fitted for lighting applications. The luminous efficiency of this white LED is 20.1 lm/W at 350 mA. The inset of Fig. 8 shows the appearance of a well-packaged LED lamp in operation. These results show that $Ca_3Si_2O_4N_2:Eu^{2+}$ could be a potential green-emitting phosphor for applications of display and illumination.

#145127 - $15.00 USD Received 31 Mar 2011; revised 27 Apr 2011; accepted 27 Apr 2011; published 28 Apr 2011

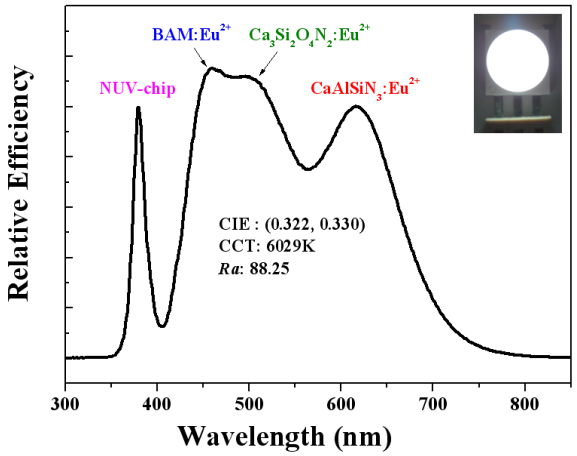

Fig. 8. EL spectra of the white LED composed of GaN-based n-UV-LED (380 nm) and $BaMgAl_{10}O_{17}:Eu^{2+}$ (blue), $Ca_3Si_2O_4N_2:Eu^{2+}$ (green) and $CaAlSiN_3:Eu^{2+}$ (red) phosphors driven by a 350-*m*A current.

4. Conclusion

Eu^{2+}-doped nitridosilicate phosphors, $Ca_3Si_2O_4N_2:Eu^{2+}$, for application in white LEDs have been successfully synthesized by a solid-state reaction. The $Ca_3Si_2O_4N_2:Eu^{2+}$ phosphor exhibited excellent luminescent properties and good thermal stability. The critical transfer distance between Eu^{2+} ions in $Ca_3Si_2O_4N_2$ was estimated to be 30.08 Å. Furthermore, the white LEDs developed in this study exhibit a high color-rendering index of 88.25. Therefore, $Ca_3Si_2O_4N_2:Eu^{2+}$ is proposed to be a promising candidate for use in white LEDs.

Acknowledgments

The authors would like to thank for the financial support from Industrial Technology Research Institute under contract no. A301AR4150, the NSC (contract no. 97-2113-M-002-012-MY3 and 97-3114-M-002-005), and the Economic Affair (contract no. 97-EC-17-A-07-S1-043).

#145127 - $15.00 USD Received 31 Mar 2011; revised 27 Apr 2011; accepted 27 Apr 2011; published 28 Apr 2011